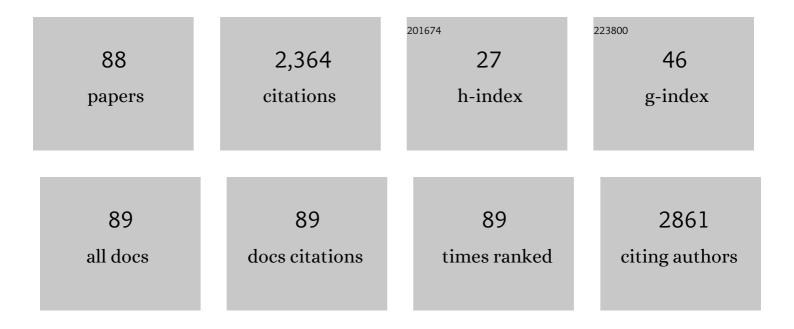
List of Publications by Year in descending order

Source: https://exaly.com/author-pdf/1307508/publications.pdf Version: 2024-02-01



ΟΠΑΝΤΙΠ

| # | Article | IF | CITATIONS |
|----|---|-----|-----------|
| 1 | Laser-Induced Surface Acoustic Wave Sensing-Based Malaria Parasite Detection and Analysis. IEEE Transactions on Instrumentation and Measurement, 2022, 71, 1-9. | 4.7 | 12 |
| 2 | Optical coherence tomography-guided confocal Raman microspectroscopy for rapid measurements in tissues. Biomedical Optics Express, 2022, 13, 344. | 2.9 | 2 |
| 3 | Cell Membrane-Coated Electrospun Fibers Enhance Keratinocyte Growth through Cell-Type Specific Interactions. ACS Applied Bio Materials, 2021, 4, 4079-4083. | 4.6 | 5 |
| 4 | A Modified Least-Squares Method for Quantitative Analysis in Raman Spectroscopy. IEEE Journal of Selected Topics in Quantum Electronics, 2021, 27, 1-9. | 2.9 | 2 |
| 5 | Towards malaria field diagnosis based on surface-enhanced Raman scattering with on-chip sample preparation and near-analyte nanoparticle synthesis. Sensors and Actuators B: Chemical, 2021, 343, 130162. | 7.8 | 1 |
| 6 | Fast hydrothermal co-liquefaction of corn stover and cow manure for biocrude and hydrochar production. Bioresource Technology, 2021, 340, 125630. | 9.6 | 19 |
| 7 | Compressive Optical Spectrometry Based on Sequency-Ordered Hadamard Transform. IEEE Photonics Journal, 2020, 12, 1-8. | 2.0 | 3 |
| 8 | Surface Enhanced Raman Spectroscopy Based Biosensor with a Microneedle Array for Minimally Invasive <i>In Vivo</i> Glucose Measurements. ACS Sensors, 2020, 5, 1777-1785. | 7.8 | 69 |
| 9 | Denoising Raman spectra by Wiener estimation with a numerical calibration dataset. Biomedical Optics Express, 2020, 11, 200. | 2.9 | 6 |
| 10 | Graphene quantum dot based chargeâ€reversal nanomaterial for nucleusâ€targeted drug delivery and efficiency controllable photodynamic therapy. Journal of Biophotonics, 2019, 12, e201800367. | 2.3 | 42 |
| 11 | Improving Depth Sensitive Fluorescence Spectroscopy With Wavefront Shaping by Spectral and Spatial Filtering. IEEE Access, 2019, 7, 170192-170198. | 4.2 | 4 |
| 12 | Depth sensitive Raman spectroscopy for skin wounds in rodents. , 2019, , . | | 0 |
| 13 | Improving depth sensitive fluorescence spectroscopy with wavefront shaping. , 2019, , . | | 0 |
| 14 | Depth-sensitive Raman spectroscopy for skin wound evaluation in rodents. Biomedical Optics Express, 2019, 10, 6114. | 2.9 | 5 |
| 15 | A Fast Fluorescence Background Suppression Method for Raman Spectroscopy Based on Stepwise Spectral Reconstruction. IEEE Access, 2018, 6, 67709-67717. | 4.2 | 13 |
| 16 | Theranostic Colloidal Nanoparticles of Pyrrolopyrrole Cyanine Derivatives for Simultaneous Near-Infrared Fluorescence Cancer Imaging and Photothermal Therapy. ACS Applied Bio Materials, 2018, 1, 1109-1117. | 4.6 | 15 |
| 17 | Hadamard transform-based calibration method for programmable optical filters based on digital micro-mirror device. Optics Express, 2018, 26, 19563. | 3.4 | 7 |
| 18 | Fast wide-field Raman spectroscopic imaging based on multi-channel narrow-band imaging and Wiener estimation. , 2018, , . | | 0 |

| # | Article | IF | CITATIONS |
|----|--|-----|-----------|
| 19 | Surface enhanced Raman spectroscopy for malaria diagnosis and intradermal measurements. , 2018, , . | | 0 |
| 20 | Sustained and Cost Effective Silver Substrate for Surface Enhanced Raman Spectroscopy Based Biosensing. Scientific Reports, 2017, 7, 6917. | 3.3 | 37 |
| 21 | Efficiency enhancement of Raman microspectroscopy at long working distance by parabolic reflector. , 2017, , . | | Ο |
| 22 | Spectral diffuse reflectance and autofluorescence imaging can perform early prediction of blood vessel occlusion in skin flaps. Journal of Biophotonics, 2017, 10, 1665-1675. | 2.3 | 9 |
| 23 | Efficiency enhancement of Raman spectroscopy at long working distance by parabolic reflector. Biomedical Optics Express, 2017, 8, 5243. | 2.9 | 3 |
| 24 | Stepwise method based on Wiener estimation for spectral reconstruction in spectroscopic Raman imaging. Optics Express, 2017, 25, 1005. | 3.4 | 34 |
| 25 | Snapshot depth sensitive Raman spectroscopy in layered tissues. Optics Express, 2016, 24, 28312. | 3.4 | 13 |
| 26 | Towards ultrasensitive malaria diagnosis using surface enhanced Raman spectroscopy. Scientific Reports, 2016, 6, 20177. | 3.3 | 48 |
| 27 | Towards field malaria diagnosis using surface enhanced Raman spectroscopy. , 2016, , . | | 1 |
| 28 | Fast wide-field Raman spectroscopic imaging based on simultaneous multi-channel image acquisition and Wiener estimation. Optics Letters, 2016, 41, 2783. | 3.3 | 18 |
| 29 | Investigation on the potential of Mueller matrix imaging for digital staining. Journal of Biophotonics, 2016, 9, 364-375. | 2.3 | 24 |
| 30 | Review of Surface Enhanced Raman Spectroscopy for Malaria Diagnosis and a New Approach for the Detection of Single Parasites in the Ring Stage. IEEE Journal of Selected Topics in Quantum Electronics, 2016, 22, 179-187. | 2.9 | 13 |
| 31 | Investigation of surface enhanced Raman spectroscopy for hemozoin detection in malaria diagnosis. , 2016, , . | | 1 |
| 32 | Early detection and differentiation of venous and arterial occlusion in skin flaps using visible diffuse reflectance spectroscopy and autofluorescence spectroscopy. Biomedical Optics Express, 2016, 7, 570. | 2.9 | 11 |
| 33 | A Method to Create a Universal Calibration Dataset for Raman Reconstruction Based on Wiener Estimation. IEEE Journal of Selected Topics in Quantum Electronics, 2016, 22, 164-170. | 2.9 | 6 |
| 34 | Polarized Raman spectroscopy for enhanced quantification of protein concentrations in an aqueous mixture. Journal of Raman Spectroscopy, 2015, 46, 744-749. | 2.5 | 3 |
| 35 | Synthesis and in vivo magnetic resonance imaging evaluation of biocompatible branched copolymer nanocontrast agents. International Journal of Nanomedicine, 2015, 10, 5895. | 6.7 | 9 |
| 36 | Dual functions of gold nanorods as photothermal agent and autofluorescence enhancer to track cell death during plasmonic photothermal therapy. Cancer Letters, 2015, 357, 152-159. | 7.2 | 40 |

| # | Article | IF | CITATIONS |
|----|--|-----|-----------|
| 37 | Non-invasive controlled release from gold nanoparticle integrated photo-responsive liposomes through pulse laser induced microbubble cavitation. Colloids and Surfaces B: Biointerfaces, 2015, 126, 569-574. | 5.0 | 29 |
| 38 | Review of Fluorescence Suppression Techniques in Raman Spectroscopy. Applied Spectroscopy Reviews, 2015, 50, 387-406. | 6.7 | 201 |
| 39 | A narrow-bandgap benzobisthiadiazole derivative with high near-infrared photothermal conversion efficiency and robust photostability for cancer therapy. Chemical Communications, 2015, 51, 4223-4226. | 4.1 | 45 |
| 40 | Gold nanorods as photothermal agents and autofluorescence enhancer to track cell death during plasmonic photothermal therapy. , 2015, , . | | 0 |
| 41 | Hollow agarose microneedle with silver coating for intradermal surface-enhanced Raman measurements: a skin-mimicking phantom study. Journal of Biomedical Optics, 2015, 20, 061102. | 2.6 | 23 |
| 42 | Optimization of advanced Wiener estimation methods for Raman reconstruction from narrow-band measurements in the presence of fluorescence background. Biomedical Optics Express, 2015, 6, 2633. | 2.9 | 18 |
| 43 | Fast photoacoustic-guided depth-resolved Raman spectroscopy: a feasibility study. Optics Letters, 2015, 40, 3568. | 3.3 | 23 |
| 44 | Gold nanorods as photothermal agents and autofluorescence enhancer to track cell death during plasmonic photothermal therapy. , 2015, , . | | 0 |
| 45 | Comparison of cone and cone shell configuration for depth sensitive fluorescence measurements in turbid media. , 2014, , . | | О |
| 46 | Recovery of Raman spectra with low signal-to-noise ratio using Wiener estimation. Optics Express, 2014, 22, 12102. | 3.4 | 66 |
| 47 | Towards <i>in vivo</i> intradermal surface enhanced Raman scattering (SERS) measurements: silver coated microneedle based SERS probe. Journal of Biophotonics, 2014, 7, 683-689. | 2.3 | 36 |
| 48 | Sequential weighted Wiener estimation for extraction of key tissue parameters in color imaging: a phantom study. Journal of Biomedical Optics, 2014, 19, 127001. | 2.6 | 4 |
| 49 | Roles of linear and circular polarization properties and effect of wavelength choice on differentiation between <i>ex vivo</i> normal and cancerous gastric samples. Journal of Biomedical Optics, 2014, 19, 046020. | 2.6 | 50 |
| 50 | Investigation of magnetic field enriched surface enhanced resonance Raman scattering performance using Fe ₃ O ₄ @Ag nanoparticles for malaria diagnosis. Proceedings of SPIE, 2014, , . | 0.8 | 0 |
| 51 | Early Prediction of Skin Viability Using Visible Diffuse Reflectance Spectroscopy and Autofluorescence Spectroscopy. Plastic and Reconstructive Surgery, 2014, 134, 240e-247e. | 1.4 | 14 |
| 52 | Phantom validation of Monte Carlo modeling for noncontact depth sensitive fluorescence measurements in an epithelial tissue model. Journal of Biomedical Optics, 2014, 19, 085006. | 2.6 | 7 |
| 53 | Raman Spectroscopy Based Techniques in Tissue Engineering—An Overview. Applied Spectroscopy Reviews, 2014, 49, 513-532. | 6.7 | 20 |
| 54 | Multifocal noncontact color imaging for depth-sensitive fluorescence measurements of epithelial cancer. Optics Letters, 2014, 39, 3250. | 3.3 | 5 |

| # | Article | IF | CITATIONS |
|----|---|-----|-----------|
| 55 | Optimization of Fe3O4@Ag nanoshells in magnetic field-enriched surface-enhanced resonance Raman scattering for malaria diagnosis. Analyst, The, 2013, 138, 6494-6500. | 3.5 | 32 |
| 56 | Fast reconstruction of Raman spectra from narrowâ€band measurements based on Wiener estimation. Journal of Raman Spectroscopy, 2013, 44, 875-881. | 2.5 | 25 |
| 57 | Axicon lens-based cone shell configuration for depth-sensitive fluorescence measurements in turbid media. Optics Letters, 2013, 38, 2647. | 3.3 | 21 |
| 58 | Optimization in interstitial plasmonic photothermal therapy for treatment planning. Medical Physics, 2013, 40, 103301. | 3.0 | 36 |
| 59 | Review of Monte Carlo modeling of light transport in tissues. Journal of Biomedical Optics, 2013, 18, 050902. | 2.6 | 253 |
| 60 | Fast depth-sensitive fluorescence measurements in turbid media using cone shell configuration. Journal of Biomedical Optics, 2013, 18, 110503. | 2.6 | 8 |
| 61 | Numerical and experimental investigation of lens based configurations for depth sensitive optical measurements. , 2013, , . | | 0 |
| 62 | Comparison of principal component analysis and biochemical component analysis in Raman spectroscopy for the discrimination of apoptosis and necrosis in K562 leukemia cells. Optics Express, 2012, 20, 22158. | 3.4 | 127 |
| 63 | Comparison of principal component analysis and biochemical component analysis in Raman spectroscopy for the discrimination of apoptosis and necrosis in K562 leukemia cells: errata. Optics Express, 2012, 20, 25041. | 3.4 | 16 |
| 64 | Numerical investigation of lens based setup for depth sensitive diffuse reflectance measurements in an epithelial cancer model. Optics Express, 2012, 20, 29807. | 3.4 | 16 |
| 65 | Hybrid method for fast Monte Carlo simulation of diffuse reflectance from a multilayered tissue model with tumor-like heterogeneities. Journal of Biomedical Optics, 2012, 17, 010501. | 2.6 | 18 |
| 66 | Modified Wiener estimation of diffuse reflectance spectra from RGB values by the synthesis of new colors for tissue measurements. Journal of Biomedical Optics, 2012, 17, 030501. | 2.6 | 44 |
| 67 | Fast reconstruction of Raman spectra from narrow-band measurements based on Wiener estimation. , 2012, , . | | 0 |
| 68 | A hybrid method for fast Monte Carlo simulation of diffuse reflectance from a multi-layered tissue model with tumor-like heterogeneities. , 2012, , . | | 0 |
| 69 | Magnetic field enriched surface enhanced resonance Raman spectroscopy for early malaria diagnosis. Journal of Biomedical Optics, 2012, 17, 017005. | 2.6 | 68 |
| 70 | Validity of the semi-infinite tumor model in diffuse reflectance spectroscopy for epithelial cancer diagnosis: a Monte Carlo study. Optics Express, 2011, 19, 17799. | 3.4 | 23 |
| 71 | Role of optical spectroscopy using endogenous contrasts in clinical cancer diagnosis. World Journal of Clinical Oncology, 2011, 2, 50. | 2.3 | 42 |
| 72 | Compact point-detection fluorescence spectroscopy system for quantifying intrinsic fluorescence redox ratio in brain cancer diagnostics. Journal of Biomedical Optics, 2011, 16, 037004. | 2.6 | 51 |

| # | Article | IF | CITATIONS |
|----|--|-----|-----------|
| 73 | Investigation of Synchronous Fluorescence Method in Multicomponent Analysis in Tissue. IEEE Journal of Selected Topics in Quantum Electronics, 2010, 16, 927-940. | 2.9 | 23 |
| 74 | Malaria diagnosis using magnetic nanoparticles. , 2010, , . | | 0 |
| 75 | Validity of the semi-infinite tumor model in tissue optics: A Monte Carlo study. , 2010, , . | | 1 |
| 76 | Spectral filtering modulation method for estimation of hemoglobin concentration and oxygenation based on a single fluorescence emission spectrum in tissue phantoms. Medical Physics, 2009, 36, 4819-4829. | 3.0 | 26 |
| 77 | Modeling of nonphase mechanisms in ultrasonic modulation of light propagation. Applied Optics, 2008, 47, 3619. | 2.1 | 7 |
| 78 | A scaling Monte Carlo method for diffuse reflectance computation from multi-layered media. , 2007, , . | | 1 |
| 79 | Scaling method for fast Monte Carlo simulation of diffuse reflectance spectra from multilayered turbid media. Journal of the Optical Society of America A: Optics and Image Science, and Vision, 2007, 24, 1011. | 1.5 | 63 |
| 80 | Development of a synchronous fluorescence imaging system and data analysis methods. Optics Express, 2007, 15, 12583. | 3.4 | 29 |
| 81 | Sequential estimation of optical properties of a two-layered epithelial tissue model from depth-resolved ultraviolet-visible diffuse reflectance spectra. Applied Optics, 2006, 45, 4776. | 2.1 | 70 |
| 82 | Angled probe design for scattering measurements from a small tissue volume. , 2006, , . | | 0 |
| 83 | Investigation of fiber-optic probe designs for optical spectroscopic diagnosis of epithelial pre-cancers. Lasers in Surgery and Medicine, 2004, 34, 25-38. | 2.1 | 65 |
| 84 | Experimental proof of the feasibility of using an angled fiber-optic probe for depth-sensitive fluorescence spectroscopy of turbid media. Optics Letters, 2004, 29, 2034. | 3.3 | 50 |
| 85 | Monte Carlo based inverse model of diffuse reflectance for determination of UV-VIS optical properties and its application to breast cancer diagnosis. , 2004, , . | | 0 |
| 86 | Effect of fiber optic probe geometry on depth-resolved fluorescence measurements from epithelial tissues: a Monte Carlo simulation. Journal of Biomedical Optics, 2003, 8, 237. | 2.6 | 84 |
| 87 | Experimental validation of Monte Carlo modeling of fluorescence in tissues in the UV-visible spectrum. Journal of Biomedical Optics, 2003, 8, 223. | 2.6 | 83 |
| 88 | Relationship between depth of a target in a turbid medium and fluorescence measured by a variable-aperture method. Optics Letters, 2002, 27, 104. | 3.3 | 66 |